A surface wave radar simulator

Yannick Béniguel[1], Muriel Darces[2], Marc Hélier[2], Alain Reineix[3], Philippe Pouliguen[4]

[1] IEEA, Courbevoie, France, beniguel@ieea.fr
[2] Sorbonne Universités, UPMC Univ. Paris 06, UR2, L2E, Paris, France, muriel.darces@upmc.fr,marc.helier@upmc.fr
[3] XLIM Institute, University of Limoges, France, alain.reineix@xlim.fr
[4] DGA/DS/MRIS, Paris, France, philippe.pouliguen@intradef.gouv.fr

***Abstract*— This paper deals with the problem of HF surface wave radar. The goal is to integrate in a unique tool the antenna radiation and the propagation calculations in order to make the analysis consistent.**

***Index Terms*—HF, surface wave radar, near field, far field**

I. INTRODUCTION

This paper addresses the problem of the surface wave (SW) radar. This kind of radar, usually operating in the HF band, has a growing interest in many applications, in particular for the survey of the coastal maritime sectors. Contrary to the sky waves, also radiated by a HF radar, the surface or ground waves decays as the square root of the distance to the source. As a result, and with a reasonable transmitted power, the signal can be propagated over hundreds of kilometers. Such a propagation mode complements the sky wave pattern of HF radars, which shows a blind zone up to the first ionosphere reflection distance.

To fully characterize the problem, both the antenna characterization and matching, the near field pattern and the propagation problem have been addressed. The antenna current distribution has been calculated using the integral equation technique. Two numerical approaches to properly take the interface into account were developed concurrently. One advantage of the technique is to isolate the ground wave contribution and estimate the related radiated power.

Another approach to the antenna problem consists in using a near field - far field transformation using measurements. A HF antenna is usually located above the ground and may reach dimensions up to 15 m height. As the ground interface is part of the radiating structure, this puts some constraints on the measurement setup. A specific equipment has been studied for this purpose. The corresponding virtual magnetic currents distribution allows calculating the field radiated at any point in the outer space.

The ground wave propagation over an irregular, inhomogeneous terrain can be derived using the parabolic equation. The problem is an initial value problem with the ground wave field contribution acting as a driver, as the sky wave has no contribution in the interface plane. Two techniques were developed concurrently. The first one uses the classical split step technique while the second is based on a finite difference scheme.

II. THE ANTENNA PROBLEM

As derived by Michalski [1], there are three different ways to write the Lorentz gauge relationship in order to meet the boundary conditions on the interface. Although equivalent from a theoretical point of view, his formulation C is the most convenient as regards its numerical implementation. This formulation has been used in the present development. With respect to the Electric Field Integral Equation (EFIE), the new equation, named Mixed Potential Integral Equation (MPIE), includes additional terms to take the Green's function modification into account.

The MPIE integral terms all involve the so-called Sommerfeld integrals. Two techniques can be used for their numerical evaluation, either the Phase Stationary Technique (PST) or the Complex Image Technique (CIT). These two techniques have been developed simultaneously.

The phase stationary technique is the classical one. It consists in finding the steepest descent contour in the k_ρ complex plane. The complex image technique takes benefit from the easiness to consider images in a method of moments procedure. The aim of the calculation consists in representing the MPIE integral terms by a sum of terms, each of them being amenable to a Weyl like integral term. The integration is performed in the k_z complex plane. The integration contour is linear in this plane. Figure 1 shows a comparison of the E_z contribution of a vertical Electric Dipole (VED) obtained with the two techniques. The agreement between the two results is excellent.

In addition to the contour contribution, the result shall integrate the poles contribution. The corresponding terms are the surface wave radiated by the HF antenna.

Again, the comparison between the two techniques has been performed. For the phase stationary technique, none of the poles are located inside the integration contour. However they are very close to it. As a result in order to make the calculation numerically tractable, it is necessary to remove their contribution in the integrand to get a regular function. It is subsequently reintroduced and calculated separately. This is the so-called modified saddle point calculation technique. For the complex image technique, all poles of the function should be included irrespective of their sign.

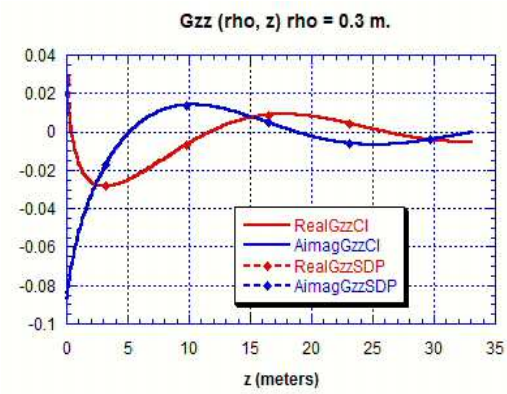

Figure 1: Comparison of the electric field vertical component contributions due to a vertical dipole

Summary

For its implementation in a method of moments code, the Sommerfeld integral terms shall give accurate results whatever the problem parameters such as the frequency, the distances and the electrical medium parameters are. To this respect, the complex image might be the most convenient technique, as accurate developments can be used for the critical values in the integration complex plane, namely when k_ρ and ρ tend to zero. For the surface wave contribution, an analytical solution involving the error function, can be derived using the modified saddle point technique.

One example of results is presented hereafter using the developed software [2]. The case considered is a typical biconical antenna of 7 meters height placed on the ground (relative dielectric constant 15 and conductivity 0.05 S / m). The calculation provides the VSWR, the currents and the fields (near field, far field and ground wave).

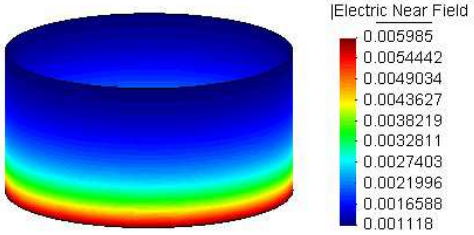

Figure 2: The near field radiated by the antenna on a cylindrical surface of radius 100 meters.

Figure 2 shows the near field pattern on a cylindrical surface containing the antenna. The major contribution comes from the ground wave. It decreases very rapidly with the altitude and as the inverse of the square root of the radial distance to the antenna for an observation point at the air ground interface.

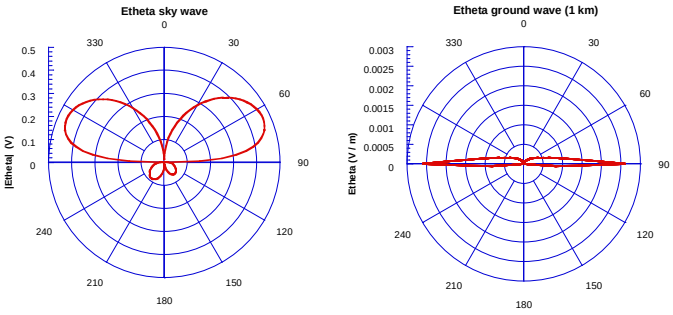

Figure 3 : sky wave and ground wave patterns

Figure 3 shows the sky wave and ground wave patterns of the HF antenna. It can be derived that the sky wave has no contribution in the interface plane. On the contrary the ground wave pattern reaches its maximum on this interface plane. Another benefit of the calculation performed for the ground wave calculation is the ability to get the radiating power. For the two propagation modes, this calculation can be done analytically. The ground wave radiated power is usually much smaller than the sky wave radiated power. However one benefit of the approach could be to include an optimization tool and put the ground wave radiated power in a cost function in order to maximize it.

III. NEAR FIELD TO FAR FIELD TRANSFORMATION

The near field to far field transformation uses equivalent sources. The antenna is replaced by a set of electric dipoles whose radiated field is identical to the real antenna radiated field. Two techniques to find the source distribution (number of dipoles, location and moment) were investigated:

- In the first one, the set of dipoles is distributed on a volume surrounding the antenna.
- The second one uses a pre – determined set of dipoles and consists in a dissemination technique to eliminate as many of them as possible and find the characteristics of the remaining distribution.

In the two cases, the knowledge of the antenna radiated near field is required. This near field may be obtained either using a numerical approach such as the one presented in the previous section [2] or using measurements. This second approach was developed at L2E.

Measurement based technique

The innovative point brought by this new method is the use, as dipole's radiation functions, of the analytic formulations developed by Norton and extended by Bannister [3] to the very near field zone. These formulations include both the sky wave and the surface wave contributions of the electromagnetic field radiated by each elementary dipole.

The experimental set up is shown on Figure 4 with the two required surfaces corresponding to the equivalent source distribution surface radiating the required field on the measurement surface.

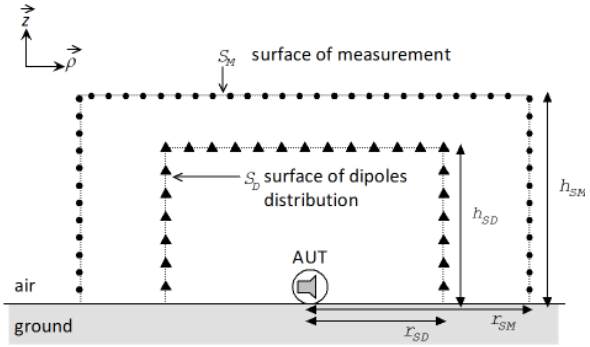

Figure 4: Experimental set up

The number of measured points is N_M. The virtual surface S_D is included inside the surface S_M (Fig. 4). The number of mesh points is N_D. At each point, three elementary electric dipoles are arranged in order to form an orthogonal basis aligned with the cylindrical basis vectors. The method states that, at each point of the surface S_M, the electromagnetic field, is equal to the sum of all the contributions coming from each of the $3N_D$ dipoles distributed over surface S_D. This leads to the following matrix equation:

$$\begin{bmatrix} \boldsymbol{D_E} \\ \boldsymbol{D_H} \end{bmatrix} [\boldsymbol{P_{S_D}}] = \begin{bmatrix} \boldsymbol{E_{S_M}} \\ \boldsymbol{H_{S_M}} \end{bmatrix} \quad (1)$$

where $\boldsymbol{E_{S_M}}$ and $\boldsymbol{H_{S_M}}$ denote the electric and magnetic vectors of size $3N_M$, measured at each point on the surface $\boldsymbol{S_M}$. $\boldsymbol{D_E}$ and $\boldsymbol{D_H}$ are respectively the electric and magnetic radiation matrices (issued from the Norton/Bannister formulations), of size $3N_M \, x \, 3N_D$, concerning the $3N_D$ electric (horizontal and vertical) dipoles located at each point of the surface S_D. $\boldsymbol{P_{SD}}$ is the unknown vector, of size $3N_D$, containing the electric moments of the previous dipoles.

Equation (1) is solved by inversion of the matrix $\begin{bmatrix} \boldsymbol{D_E} \\ \boldsymbol{D_H} \end{bmatrix}$ in order to compute the vector $\boldsymbol{P_{DS}}$. The accuracy of the inversion depends on the actual number of dipoles contributing to the radiation. More precisely, the idea is to unselect the dipoles that have a non-significant contribution to the total field. To achieve this objective, the inversion is carried out by applying the singular value decomposition (SVD) to the matrix $\begin{bmatrix} \boldsymbol{D_E} \\ \boldsymbol{D_H} \end{bmatrix}$ associated with a threshold power criterion (Fig. 5).

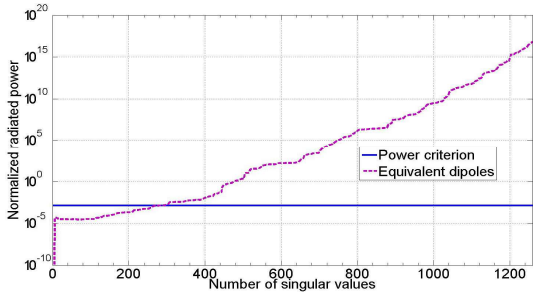

Fig. 5 Power radiated by the equivalent dipoles vs. singular values.

This criterion is linked to the total power radiated by the AUT, in the near field zone, and is calculated from the measurement of the electromagnetic field on surface S_M. Then, the singular value matrix is scanned and truncated by decreasing the order until the corresponding calculated power reaches this power criterion. Once the vector $\boldsymbol{P_{SD}}$ is determined, the electric far field can be easily computed. In order to perform the SVD, we need to know both the electric and magnetic fields. However, to avoid measuring the magnetic field, it is possible to approximate it, based on the plane wave assumption, and still apply the power criterion.

A. Results

The first example is a quarter-wave monopole working at 10 MHz and located above a moist soil ($\varepsilon_r = 13$ and $\sigma = 0.05$ S.m^{-1}). The near-field data are obtained from CST MWS. Fig. 6 shows the amplitude and phase of the electric field extracted from CST MWS and the one calculated using to the NF/FF transformation. As can be seen, the electric near field is well reconstituted.

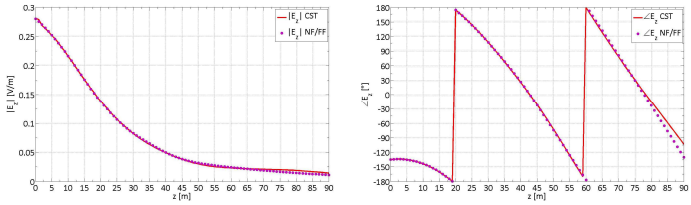

(a) (b)

Fig. 6. Electric near field over a generating line of the cylinder: (a) magnitude, (b) phase.

Far field

CST MWS does not take into account the surface wave in the far field zone, but the results obtained by means of the SVD method have already been compared to the results obtained with NEC/SOMNEC and are satisfactory. $\boldsymbol{E_\theta}$ is the far field component of the electric field determined after a SVD considering both the electric and magnetic near fields, and $\boldsymbol{E_\theta}$' is the far field component of the electric field determined after

the SVD, from the electric near field only. At a distance of 10λ from the antenna, we can see on the left panel of Figure 7 that the surface wave ($\theta \approx 90$ °) is predominant. But at 100λ from the antenna, the sky wave is predominant, and reaches its maximum magnitude at $\theta \approx 70$.

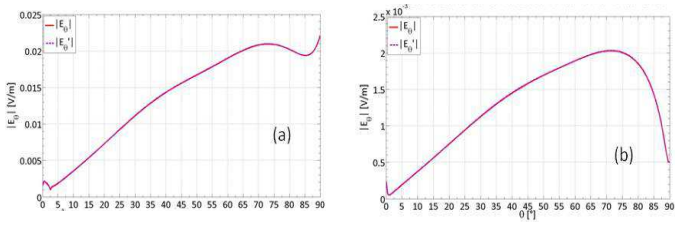

Figure 7: Radiated electric field at 10λ (left panel) and 100λ (right panel).

This technique allowing predicting the far field, including the ground wave, from a near field measurement has been verified building the experimental set up shown on Figure 4.

IV. PROPAGATION

In order to be able to cross check the results, the propagation calculation was done by two approaches: using a multiple phase screen technique and using a finite difference technique. These two techniques solve the parabolic equation which is derived from the Helmholtz equation using the paraxial approximation. This approximation assumes than the field variation along the line of sight (LOS) is much smaller than its variation in the transverse to the LOS plane. This approximation reduces the validity domain to angles smaller than 15° from the LOS. It is always verified for a ground wave radar. To be noticed that including higher order terms in the equation allows extending its validity angles range to angles up to 45°. The two techniques developed solve a 2D problem, marching on in space from the source location to a given observation point. The field is calculated on vertical lines with respect to the mean tangent plane.

From a numerical point of view, this is an initial value problem with two specific boundary conditions: at the interface and on top of the domain. These boundary conditions are met differently by the two techniques developed as indicated hereafter. The initial field is the solution of the antenna problem. It may result either from the use of a numerical technique or from a near field to far field transformation. It shall be noticed that only the surface wave shall be considered as it can be demonstrated that the sky wave has no contribution in the air - ground interface plane. The antenna analysis integral equation technique, presented at section II allows isolating this contribution.

The multiple phase screen technique takes advantage of the fact that the parabolic equation reduces to an ordinary differential equation when using a Fourier transformation from the space domain to the *kz* domain where *kz* is the vertical component of the wave number. The algorithm alternates two calculations at each space step: the Fourier transform calculation and the differential equation calculation. The first one allows considering the scattering effects and the second one the field modification due to the propagation along the LOS. On the upper altitude of the space domain, an absorbing boundary condition has been implemented At the air - ground interface, the Leontovich conditions are implemented. The overall algorithm is very efficient allowing considering arbitrary terrain profiles and ground impedance discontinuities. The CPU time is very small, typically a few tenths of seconds for a wave propagation over 300 km.

The finite difference technique on the other hand uses a centre finite difference scheme. In this case, the center point is located between two vertical lines and this scheme leads to a tridiagonal matrix. The upper boundary condition is an adaptation of the PML first introduced by Bérenger [4]. An efficient way to introduce the PML in the FD grid is to use stretched coordinates in the vertical direction. Such an approach allows deriving the equation to be solved into the PML region.

The consistency of the results provided has been cross checked with respect to a classical problem, namely the one exhibiting the Millington effect [5]. The profile has an impedance discontinuity 86 km away from the source. After this distance, the propagation, which was previously over land, is over sea. The field attenuation shows the recovery of the field strength after crossing the discontinuity. (cf. Figure 8).

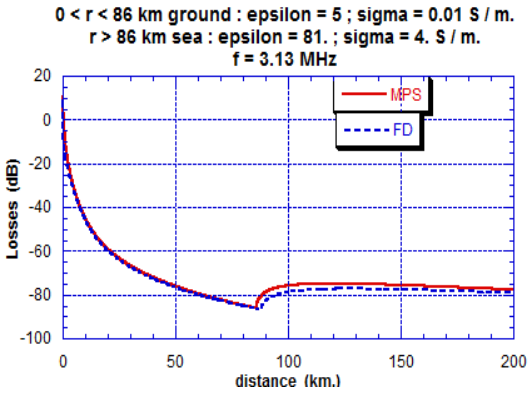

Figure 8: Field propagation on a terrain with an impedance discontinuity

V. DOPPLER EFFECT / PROPAGATION OVER THE SEA

The software developed in this study includes different terrain models. A particular attention was paid to the roughness modeling. The objective was to take into account different topologies of terrains such as mountains and plains. This has been done, using a fractal model based on the diamond square approach. A typical example is shown on the figure 9

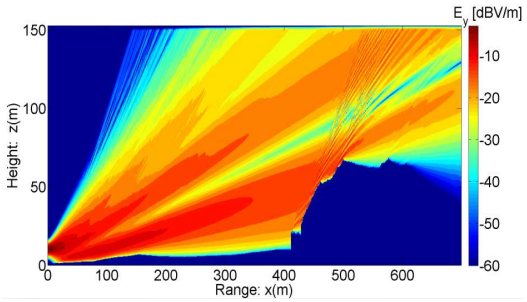

Figure 9: Modeling of the propagation of a rough terrain

As shown above, the software is able to model a rough surface on one side and an abrupt discontinuity between this surface and the ocean as shown on figure 10 on the other side. The last part consists in considering a realistic model of the sea surface, taking in particular the swell into account. Using the directional model of Pierson Moskowitz, we met this objective. This model can be considered as the summation of weighted spatial signals at different frequencies. Therefore we only have to multiply the surface height at each point along a terrain profile by a complex exponential factor to take the propagation versus time into account. The real part of the result will give different realizations of the surface.

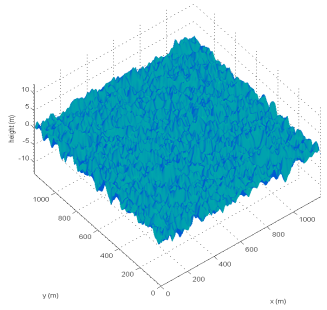

Figure 10: realization of a sea surface profile

The final calculation consists in the computation of the Doppler spectrum. To do it, a profile is extracted from a realization of the random surface. This profile is introduced in the parabolic equation software. Several realizations are considered at successive times. The backscattered field is then computed at the operating frequency. The integration over a long observation time of the moving sea gives the Doppler spectrum which exhibits the Doppler components as expected (cf Figure 11).

To obtain this result, the following steps have been performed:

- The extraction of profiles from the different realizations of the surface at different time steps,
- The calculation of the currents from the fields calculated using the parabolic equation algorithm. These currents are then considered as the sources for the backward diffracted field calculation.
- The evaluation of the field diffracted by the different realizations of the profile in the far region, each profile is calculated at one time step.
- A Fast Fourier Transformation of the successive results for the diffracted far field. They are directly related to the Doppler Spectrum.

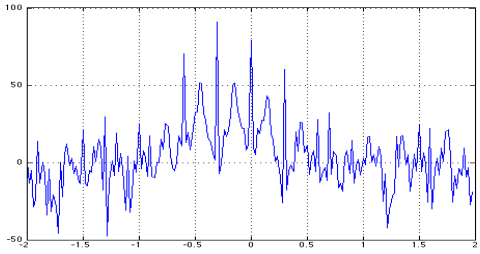

Figure 11: Observed spectrum for the input data set: f=15 MHz, λ_S=10m, dt=0.25s, T_{obs}=50s, u=3 m/s f_d=0.3 Hz

VI. CONCLUSION

Many innovative points have been considered in this study aiming to develop a global tool allowing addressing the antenna plus surface wave propagation problem. The global tool developed might support the design of surface wave radars.

ACKNOWLEDGEMENT

This study has been done in the frame of the PROPHETE project under funding of the French Research National Agency (ANR)

REFERENCES

[1] Michalski K., D. Zheng, "Electromagnetic Scattering and Radiation by Surfaces of Arbitrary Shape in Layered Media, Part I: Theory", IEEE AP, Vol 38, N° 3, 1990.

[2] http://www.ieea.fr/fr/logiciels/icare-mom.html

[3] P. Bannister, "The quasi-near fields of dipole antennas", IEEE Transactions on Antennas and Propagation, vol.15, no.5, pp. 618-626, Sept 1967

[4] J.-P. Bérenger, "A perfectly matched layer for the absorption of electromagnetic waves", J. Computational Physics, vol 114, N°1, pp 185-200, 1994

[5] G. Millington, G. Isted, « Ground wave propagation over an inhomogeneous smooth earth: part 2, experimental evidence and practical implementation", Proc. IEE, vol. 97, Pt III, pp. 209 – 221, 1950